ChemComm

COMMUNICATION

View Article Online
View Journal

Cite this: DOI: 10.1039/d1cc03857e

Received 16th July 2021,
Accepted 31st August 2021

DOI: 10.1039/d1cc03857e

rsc.li/chemcomm

Better fuels for photocatalytic micromotors: a case study of triethanolamine†

Shifang Duan, Pengzhao Xu and Wei Wang *

Efficient fuels are critical for designing photocatalytic micromotors with high performance. We discover that 0.5 mM of triethanolamine can power TiO_2–Pt motors at 35 μm s^{-1} without producing bubbles, a significant improvement over conventional fuels such as water, H_2O_2 or hydroquinone. The effectiveness of hole scavengers such as triethanolamine can be generalized to other photocatalytic micromotors containing a heterojunction with an n-type (but not a p-type) semiconductor.

Inspired by biological motors, synthetic micro- and nanomotors convert the energy stored in their environment into mechanical work, and as a result, move autonomously in fluids.[1–3] In particular, motors powered by surface photocatalysis (known as "photocatalytic micromotors")[4,5] are easy to handle and be controlled remotely, and are potentially useful in the degradation of microplastics and other organic pollutants.[6,7] However, they often suffer from low energy conversion efficiency,[8] and therefore require a high level of light intensity and fuel concentration to operate, which in turn greatly limits their usefulness in realistic scenarios.

In light of these challenges, there have been continuous efforts in designing photocatalytic micromotors that move faster and consume less fuel. One direction is to design micro- and nanomotors with better semiconductor materials[9,10] or *via* optimizing motor structures,[11,12] but this often involves complicated sample fabrication or materials. The second direction is to use fuels beyond water, such as H_2O_2,[13,14] hydroquinone/benzoquinone (H_2Q/BQ),[15,16] hydrazine,[17] glucose,[18] and urea.[19] There is a continuous need to discover new fuels that are of high performance.

In this communication, we report a new fuel, triethanolamine ("TEOA"), that powers a typical photocatalytic micromotor (TiO_2–Pt) at a speed that is 5 times that in pure water, 4 times that in H_2O_2, and 3 times that in hydroquinone (see Video S1, ESI†). Additional key advantages of TEOA include a low operating concentration, a low requirement on light intensity, mild salt tolerance, and lack of bubbles. TEOA is an effective fuel because it serves as a hole scavenger that significantly boosts the kinetics of the photoanodic half-reaction of a TiO_2–Pt micromotor,[20] a design principle that can be generically applied to other photocatalytic micromotors.

Throughout this communication, a TiO_2–Pt Janus microsphere is used as a model for a photocatalytic micromotor, which has been a popular subject of study over the years.[21–24] These Janus microspheres are fabricated by half-coating titanium dioxide (TiO_2) microspheres (1.2 ± 0.1 μm in diameter) with a layer of platinum (Pt) (Fig. 1a, see ESI† for synthesis details). Under UV light irradiation, TiO_2 generates electrons and holes that react at the surface of Pt and TiO_2, respectively (see Fig. 1b for a schematic). They then react with fuel molecules and create a self-generated electric field that propels a

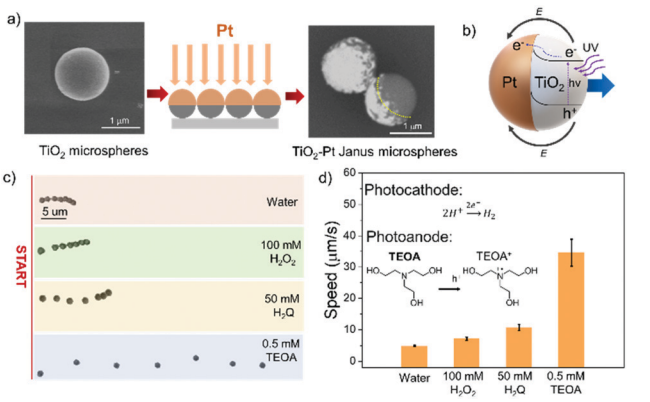

Fig. 1 Powering TiO_2–Pt micromotors with triethanolamine (TEOA). (a) Schematic of the synthesis of TiO_2–Pt Janus microspheres. (b) Self-electrophoresis mechanism that powers light-driven TiO_2–Pt micromotors. (c) 1s Trajectories of TiO_2–Pt micromotors under UV light (650 mW cm^{-2}) in different fuel solutions (taken from Video S1, ESI†). (d) Average speeds of TiO_2–Pt motor in different fuels. Error bars represent standard errors from 20 independent measurements (see ESI† for calculation details). Inset: Photocathodic and anodic half-reactions involving TEOA.

School of Materials Science and Engineering, Harbin Institute of Technology (Shenzhen), Shenzhen, Guangdong 518055, China. E-mail: weiwangsz@hit.edu.cn

† Electronic supplementary information (ESI) available. See DOI: 10.1039/d1cc03857e

micromotor away from the Pt end. This mechanism, known as self-electrophoresis,[24–26] has successfully explained the self-propulsion of photocatalytic micromotors with a metal-semiconductor heterojunction.[27,28]

A key component in this mechanism is the choice of fuel molecules. Popular choices include water, H_2O_2, and the benzoquinone (BQ)/hydroquinone (H_2Q) pair. TEOA compares favourably to all these fuel molecules in several aspects. The most prominent advantage of TEOA is its effectiveness in powering motors at high speeds. For example, as shown in Fig. 1c, the trajectories of a TiO_2–Pt micromotor are noticeably longer in 0.5 mM of TEOA than those in water, 100 mM H_2O_2, or 50 mM H_2Q (the optimal concentrations determined for each fuel, see Fig. S2, ESI†). Correspondingly, the motor speeds are highest in 0.5 mM TEOA, reaching 35 μm s^{-1} (30 body lengths per second).

Note that speeds on the order of tens of body lengths per second have been reported for TiO_2-based photocatalytic micromotors.[21,24,27,29,30] However, it is generally challenging to compare absolute speeds across different literature reports, because of possible differences in material preparation and operating conditions. As a result, speeds of TiO_2–Pt micromotors in TEOA in this communication are compared with those in H_2O_2 and H_2Q from our own labs under the same lighting conditions. Moreover, the speeds of TEOA-powered motors can potentially be further improved by optimizing their material properties[31,32] or coating composition.[33]

In addition to fast speeds, other advantages of TEOA as a fuel molecule are further quantified in Fig. 2. First, Fig. 2a shows that a TiO_2–Pt motor can self-propel in TEOA of a wide range of concentrations (10^{-2} to 10^{2} mM), reaching a peak speed at 0.5 mM of TEOA. Motor speeds decrease at higher concentrations possibly because TEOA as an organic base readily reacts with water and form ions, which are known to slow down self-electrophoretic motors.[34–36] Note that the concentration of TEOA can be as small as 0.01 mM, which is orders of magnitude smaller than typical fuels used in the literature (*e.g.*, H_2O_2 and hydrazine),[17] and of negligible toxicity to cells.[37]

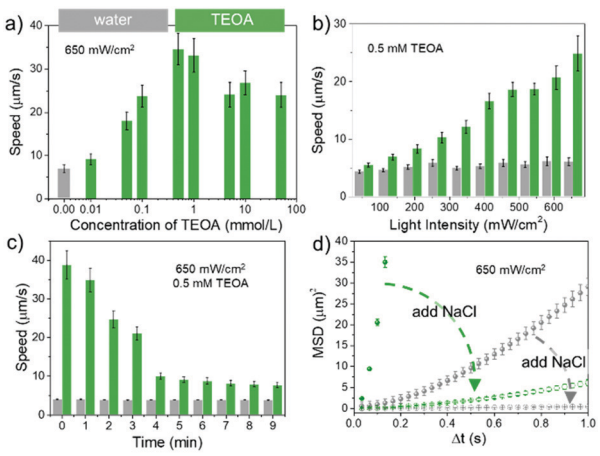

Fig. 2 Water- or TEOA-powered TiO_2–Pt micromotors under different experimental conditions. (a and b) Influence of TEOA concentrations (a) and UV light intensity (b) on motor speeds. (c) Speed of motors under continuous illumination over time. (d) The effect of adding salt (final concentration 5 mM NaCl) to TiO_2–Pt motors powered by water or 0.5 mM of TEOA. In all figures, data in pure water are coloured grey, and those in TEOA are green. Error bars represent standard errors from 20 independent measurements.

Second, Fig. 2b shows that the speeds of motors in TEOA and water both monotonically increase as light intensity increases, but the motor speed at lower light intensities (123 mW cm^{-2}) in TEOA is comparable with that at high light intensities (650 mW cm^{-2}) in water, a useful feature if low lighting is preferred (for example to minimize photobleaching of dyes). Third, similar to other fuels, motors in TEOA slow down significantly during prolonged light irradiation (Fig. 2c),[38] possibly because of the deactivation of the catalyst surface over time. However, motors in TEOA after 10 minutes still move twice as fast as those in water, a feature useful for studying their collective behaviours over a long time. Furthermore, no bubble was produced even after tens of minutes of operation or with a large motor population. This is because, instead of producing O_2, holes react with TEOA to yield $TEOA^{+}$.[39] Finally, Fig. 2d shows that the boosted performance of TEOA enables the propulsion of a TiO_2–Pt motor in ionic strength of 5 mM, whereas water-powered micromotors show Brownian motion in the same ionic strength.

The most common way for a fuel molecule to improve the performance of a photocatalytic micromotor is by accelerating the reaction and thereby increasing the photocurrent. In the particular case of TiO_2–Pt, the Pt cap not only promotes the separation of photogenerated electrons and holes, but also acts as a co-catalyst that facilitates the reaction of electrons on its surface.[40,41] TiO_2, on the other hand, is known to be a mediocre cocatalyst for oxygen evolution, and thus the consumption of photogenerated holes on the surface of TiO_2 becomes the rate-limiting step.[42,43] Therefore, to expedite this half-reaction, and thereby increasing the overall photocurrent, hole scavengers such as H_2Q,[44] H_2O_2,[45] and alcohols[46] are commonly used as fuels in photocatalytic micromotors. The same principle also applies to TEOA, which is known to be a good hole scavenger in the literature of photocatalytic hydrogen production.[47–49]

To confirm that the effectiveness of TEOA indeed stems from an increase of the photocurrent, we measured the photocurrent between a TiO_2 film and a Pt film with a typical three-electrode electrochemical cell (Fig. 3a, see ESI† for experiment details and Fig. S3 for more results). In all measurements we report below, photocurrents flow from Pt (cathode) to TiO_2 (anode), consistent with the self-electrophoresis mechanism depicted in Fig. 1d. Importantly, under UV irradiation of 650 mW cm^{-2}, we recorded a photocurrent of 2.7 mA cm^{-2} in 0.5 mM of TEOA, much larger than that acquired in 100 mM H_2O_2 (0.65 mA cm^{-2}) or 50 mM H_2Q (0.79 mA cm^{-2}). This comparison in photocurrent (Fig. 3b) also agrees nicely with that of motor speeds among different fuels, and is thus a powerful indication that the effectiveness of TEOA lies in an improvement in the reaction rate of photocatalysis on TiO_2–Pt.

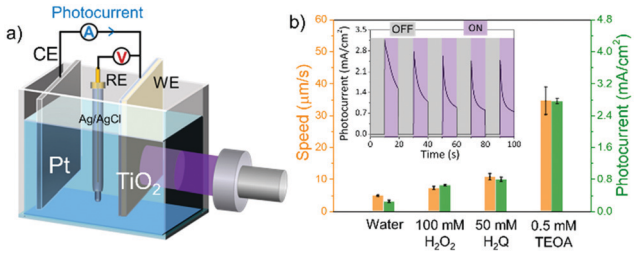

Fig. 3 Understanding the effectiveness of TEOA in powering micromotors. (a) Schematic of the electrochemical cell to measure photocurrents. (b) Comparison between photocurrents and motor speeds in different fuel solutions (speed data from Fig. 1d). Inset: Representative transient photocurrents measured in 0.5 mM TEOA under UV light (650 mW cm^{-2}). Error bars in photocurrents represent standard errors from 5 measurements.

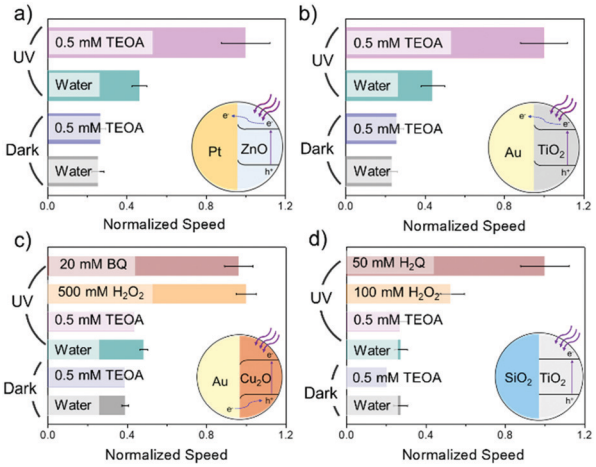

Fig. 4 Performance of different photocatalytic motors in TEOA: ZnO–Pt (a), TiO_2–Au (b), Cu_2O–Au (c), and SiO_2–TiO_2 (d) under UV light (650 mW cm^{-2}). Insets in each panel show the separation and migration of photo-carriers that follow the UV excitation for each type of micromotor. The maxima of the average speed for each figure is 11.2, 13.4, 4.7 and 10.7, respectively. Error bars represent standard errors from 20 independent measurements.

Why is TEOA such a good hole scavenger for a TiO_2–Pt micromotor? It is natural to suspect the following three aspects: quantum efficiency (*i.e.* a better separation of photoelectrons and holes), thermodynamics (*i.e.* TEOA reacts more easily with holes), or kinetics (*i.e.* TEOA consumes holes faster). The first possibility of TEOA generating more electrons and holes out of TiO_2 is unlikely, given that the fundamental material properties and light absorption of TiO_2 remain unchanged. Second, the electrochemical potential of $TEOA^+$/TEOA (+0.82 V *vs.* NHE),[50] is larger than that of O_2/H_2O_2 (+0.69 V) or BQ/H_2Q (+0.70 V), suggesting that thermodynamically TEOA is in fact a worse hole scavenger than H_2O_2 or H_2Q.

This leaves it the only possibility that TEOA improves the kinetics of the photocatalytic reaction on TiO_2–Pt. This is reasonable, because an early study shows that the oxidation of TEOA by photogenerated holes is preceded by a deprotonation process, which is a fast kinetic process that reduces the energy barrier in the electron transfer process.[51]

$$\mathrm{TEOA} \xrightarrow{-e^-} \mathrm{TEOA}^+ \xrightarrow{-e^-} (\mathrm{HOCH_2CH_2})_2\mathrm{NCH_2CHO} \quad (1-1)$$

Finally, we extend the observed improvement in speeds of TiO_2–Pt micromotors by TEOA to other photocatalytic micromotors. In Fig. 4a and b and Video S3 (ESI†), we show that both a TiO_2–Au micromotor made of coating gold (Au) instead of Pt on TiO_2 microspheres, and a ZnO–Pt micromotor made of coating Pt on zinc oxide (ZnO, also an n-type semiconductor) microspheres, show a significant boost in speeds when TEOA is present. TEOA is effective in these two cases because TiO_2–Au and ZnO–Pt, like TiO_2–Pt, contain heterojunctions between an n-type semiconductor and a metal of high work function, thus suffer from the same issue of slow consumption of photogenerated holes. Adding TEOA then accelerates this half-reaction, increases the overall reaction rate, and speeds up the motor.

TEOA is, however, not effective when hole scavengers are not useful. For example, we show in Fig. 4c that neither TEOA, nor ethanol or H_2Q, is an effective fuel for a Cu_2O–Au micromotor (Video S4, ESI†). This is because Cu_2O is a p-type semiconductor, and when forming a heterojunction with Au the electrons at the metal end will flow to the semiconductor, causing the Cu_2O/water interface to be dominated by reduction (exactly the opposite to TiO_2–Pt). To improve the performance of a Cu_2O motor, electron scavengers rather than hole scavengers are needed, which makes H_2O_2 or BQ, rather than TEOA or H_2Q, an effective fuel for Cu_2O–Au motors. Moreover, TEOA is not useful for SiO_2–TiO_2 micromotor either (Fig. 4d), made by half-coating a silicon dioxide (SiO_2) microsphere with TiO_2 (see ESI† for details on sample preparation). In this case, the photocurrent is limited not by one of the two half-reactions, but by high recombination between photoelectrons and holes. Therefore, redox shuttles such as H_2O_2 or the BQ/H_2Q pair are effective fuels for SiO_2–TiO_2 motors because they improve the reaction on both the photocathode and anode (shown in Video S5, ESI†).

In conclusion, we have demonstrated that the speed of photocatalytic TiO_2–Pt micromotors can be significantly improved by an aqueous solution containing mM triethanolamine (TEOA), reaching $\sim$35 μm s^{-1} at 0.5 mM under 650 mW cm^{-2} UV irradiation. Additional advantages of this new fuel molecule include a small operating concentration that is 4 orders of magnitude lower than other common fuels, a minimal effect of bubbles even after tens of minutes of operation or with a large motor population, as well as the ability to move in salt solutions up to 5 mM concentration. The excellent performance of TEOA as fuel for photocatalytic motors is due to its fast deprotonation as it scavenges photogenerated holes, accelerating the reaction kinetics at the TiO_2 surface. This TEOA-mediated acceleration can be extended to other photocatalytic micromotors made of n-type semiconductors (such as TiO_2 and ZnO), but not those made of p-type (*e.g.* Cu_2O) or without a metal-semiconductor interface. Beyond the discovery of a highly effective fuel molecule, this study also highlights the thermodynamic and kinetic principles in designing efficient photocatalytic micromotors.

This project is financially supported by the Science Technology and Innovation Program of Shenzhen (JCYJ20190806144807401), the National Natural Science Foundation of China (11774075) and

the Natural Science Foundation of Guangdong Province (No. 2017B030306005). We are grateful for the helpful discussions with Prof. Thomas Mallouk, Dr Pengtao Xu, Prof. Jizhuang Wang and Prof. Jinyao Tang.

Conflicts of interest

There are no conflicts to declare.

Notes and references

1 J. Wang, *Nanomachines: fundamentals and applications*, John Wiley & Sons, 2013.
2 X. Chen, C. Zhou and W. Wang, *Chem. – Asian J.*, 2019, **14**, 2388–2405.
3 W. Wang, X. Lv, J. L. Moran, S. Duan and C. Zhou, *Soft Matter*, 2020, **16**, 3846–3868.
4 J. Wang, Z. Xiong, J. Zheng, X. Zhan and J. Tang, *Acc. Chem. Res.*, 2018, **51**, 1957–1965.
5 R. Dong, Y. Cai, Y. Yang, W. Gao and B. Ren, *Acc. Chem. Res.*, 2018, **51**, 1940–1947.
6 Y. Ying and M. Pumera, *Chem. – Asian J.*, 2019, **25**, 106–121.
7 B. Jurado-Sánchez and J. Wang, *Environ. Sci.: Nano*, 2018, **5**, 1530–1544.
8 W. Wang, T.-Y. Chiang, D. Velegol and T. E. Mallouk, *J. Am. Chem. Soc.*, 2013, **135**, 10557–10565.
9 K. Villa, C. L. Manzanares Palenzuela, Z. K. Sofer, S. Matějková and M. Pumera, *ACS Nano*, 2018, **12**, 12482–12491.
10 L. Kong, C. C. Mayorga-Martinez, J. Guan and M. Pumera, *Small*, 2020, **16**, 1903179.
11 X. Wang, L. Baraban, V. R. Misko, F. Nori, T. Huang, G. Cuniberti, J. Fassbender and D. Makarov, *Small*, 2018, **14**, 1802537.
12 A. M. Pourrahimi, K. Villa, C. L. Manzanares Palenzuela, Y. Ying, Z. Sofer and M. Pumera, *Adv. Funct. Mater.*, 2019, **29**, 1808678.
13 W. F. Paxton, K. C. Kistler, C. C. Olmeda, A. Sen, S. K. Angelo, Y. Cao, T. E. Mallouk, P. E. Lammert and V. H. Crespi, *J. Am. Chem. Soc.*, 2004, **126**, 13424–13431.
14 A. A. Solovev, W. Xi, D. H. Gracias, S. M. Harazim, C. Deneke, S. Sanchez and O. G. Schmidt, *ACS Nano*, 2012, **6**, 1751–1756.
15 J. Zheng, B. Dai, J. Wang, Z. Xiong, Y. Yang, J. Liu, X. Zhan, Z. Wan and J. Tang, *Nat. Commun.*, 2017, **8**, 1–7.
16 J. Wang, Z. Xiong, X. Zhan, B. Dai, J. Zheng, J. Liu and J. Tang, *Adv. Mater.*, 2017, **29**, 1701451.
17 W. Gao, A. Pei, R. Dong and J. Wang, *J. Am. Chem. Soc.*, 2014, **136**, 2276–2279.
18 Q. Wang, R. Dong, C. Wang, S. Xu, D. Chen, Y. Liang, B. Ren, W. Gao and Y. Cai, *ACS Appl. Mater. Interfaces*, 2019, **11**, 6201–6207.
19 T. Patiño, X. Arqué, R. Mestre, L. Palacios and S. Sánchez, *Acc. Chem. Res.*, 2018, **51**, 2662–2671.
20 J. Lee, J. Kwak, K. C. Ko, J. H. Park, J. H. Ko, N. Park, E. Kim, T. K. Ahn, J. Y. Lee and S. U. Son, *Chem. Commun.*, 2012, **48**, 11431–11433.
21 L. Kong, C. C. Mayorga-Martinez, J. Guan and M. Pumera, *ACS Appl. Mater. Interfaces*, 2018, **10**, 22427–22434.
22 F. Mou, L. Kong, C. Chen, Z. Chen, L. Xu and J. Guan, *Nanoscale*, 2016, **8**, 4976–4983.
23 Y. Gao, F. Mou, Y. Feng, S. Che, W. Li, L. Xu and J. Guan, *ACS Appl. Mater. Interfaces*, 2017, **9**, 22704–22712.
24 R. Dong, Q. Zhang, W. Gao, A. Pei and B. Ren, *ACS Nano*, 2016, **10**, 839–844.
25 Y. Wang, R. M. Hernandez, D. J. Bartlett, J. M. Bingham, T. R. Kline, A. Sen and T. E. Mallouk, *Langmuir*, 2006, **22**, 10451–10456.
26 W. Wang, W. Duan, S. Ahmed, T. E. Mallouk and A. Sen, *Nano Today*, 2013, **8**, 531–554.
27 B. Jang, A. Hong, H. E. Kang, C. Alcantara, S. Charreyron, F. Mushtaq, E. Pellicer, R. Büchel, J. Sort and S. S. Lee, *ACS Nano*, 2017, **11**, 6146–6154.
28 Q. Zhang, R. Dong, Y. Wu, W. Gao, Z. He and B. Ren, *ACS Appl. Mater. Interfaces*, 2017, **9**, 4674–4683.
29 Y. Wu, R. Dong, Q. Zhang and B. Ren, *Nano-Micro Lett.*, 2017, **9**, 30.
30 C. Chen, S. Tang, H. Teymourian, E. Karshalev, F. Zhang, J. Li, F. Mou, Y. Liang, J. Guan and J. Wang, *Angew. Chem.*, 2018, **130**, 8242–8246.
31 M. Urso, M. Ussia and M. Pumera, *Adv. Funct. Mater.*, 2021, 2101510.
32 X. Ma, J. Katuri, Y. Zeng, Y. Zhao and S. Sanchez, *Small*, 2015, **11**, 5023–5027.
33 Z. Xiao, J. Chen, S. Duan, X. Lv, J. Wang, X. Ma, J. Tang and W. Wang, *Chem. Commun.*, 2020, **56**, 4728–4731.
34 J. L. Moran and J. D. Posner, *Phys. Fluids*, 2014, **26**, 042001.
35 A. Brown and W. Poon, *Soft Matter*, 2014, **10**, 4016–4027.
36 W. F. Paxton, P. T. Baker, T. R. Kline, Y. Wang, T. E. Mallouk and A. Sen, *J. Am. Chem. Soc.*, 2006, **128**, 14881–14888.
37 D. Zhang, C. Gao, R. Li, L. Zhang and J. Tian, *Arch. Pharmacal Res.*, 2017, **40**, 579–591.
38 T. Maric, M. Z. M. Nasir, M. Budanovic, O. Alduhaish, R. D. Webster and M. Pumera, *Appl. Mater. Today*, 2020, **20**, 100659.
39 F. R. Keene, C. Creutz and N. Sutin, *Coord. Chem. Rev.*, 1985, **64**, 247–260.
40 Y. Zheng, Y. Jiao, Y. Zhu, L. H. Li, Y. Han, Y. Chen, A. Du, M. Jaroniec and S. Z. Qiao, *Nat. Commun.*, 2014, **5**, 1–8.
41 J. S. Ho, A. J. Yeh, E. Neofytou, S. Kim, Y. Tanabe, B. Patlolla, R. E. Beygui and A. S. Poon, *Proc. Natl. Acad. Sci. U. S. A.*, 2014, **111**, 7974–7979.
42 I. C. Man, H. Y. Su, F. Calle-Vallejo, H. A. Hansen, J. I. Martínez, N. G. Inoglu, J. Kitchin, T. F. Jaramillo, J. K. Nørskov and J. Rossmeisl, *ChemCatChem*, 2011, **3**, 1159–1165.
43 Y. Jiao, Y. Zheng, M. Jaroniec and S. Z. Qiao, *Chem. Soc. Rev.*, 2015, **44**, 2060–2086.
44 D.-G. Wu, C.-H. Huang, L.-B. Gan, W. Zhang, J. Zheng, H. X. Luo and N. Q. Li, *J. Phys. Chem. B*, 1999, **103**, 4377–4381.
45 B. Abramović, V. Despotović, D. Šojić and N. Finčur, *React. Kinet., Mech. Catal.*, 2015, **115**, 67–79.
46 S. Kaneco, Y. Shimizu, K. Ohta and T. Mizuno, *J. Photochem. Photobiol., A*, 1998, **115**, 223–226.
47 W. Zhang, J. Hong, J. Zheng, Z. Huang, J. Zhou and R. Xu, *J. Am. Chem. Soc.*, 2011, **133**, 20680–20683.
48 X. Zhang, T. Peng, L. Yu, R. Li, Q. Li and Z. Li, *ACS Catal.*, 2015, **5**, 504–510.
49 Y. Liu, Y.-H. Li, X. Li, Q. Zhang, H. Yu, X. Peng and F. Peng, *ACS Nano*, 2020, **14**, 14181–14189.
50 A. Rodenberg, M. Orazietti, B. Probst, C. Bachmann, R. Alberto, K. K. Baldridge and P. Hamm, *Inorg. Chem.*, 2015, **54**, 646–657.
51 Y. J. Yuan, Z. T. Yu, X. Y. Chen, J. Y. Zhang and Z. G. Zou, *Chem. – Asian J.*, 2011, **17**, 12891–12895.

